QUICK AND AFFORDABLE SCAL: SPONTANEOUS CORE ANALYSIS

M. A. Fernø[a], Å .Haugen[b], B. Brattekås[a,c], G. Mason[d] and N. Morrow[d]
[a] Dept. of Physics and Technology, University of Bergen, Norway
[b] Statoil, Bergen, Norway; [c] The National IOR centre, Dept. of Petroleum Technology, University of Stavanger; [d] Dept. of Chemical & Petroleum Engineering, University of Wyoming, USA

This paper was prepared for presentation at the International Symposium of the Society of Core Analysts held in St. John's Newfoundland and Labrador, Canada, 16-21 August, 2015

ABSTRACT

We present a quick and affordable special core analysis method that uses spontaneous imbibition to estimate absolute permeability, capillary pressure and relative permeability. The method uses the two-ends-open free (TEO-free) boundary condition where one end of the core is in brine and the other in oil. Counter-current and co-current flow are easily measured and quantified and from them we estimate end-point relative permeability and capillary pressure using, by most oil recovery standards, very simple analysis. The analysis is based on an assumption of a piston-like displacement and includes the capillary back pressure at the open face. Piston-like displacement was verified using *in-situ* imaging by positron-emission-tomography (PET) to visualize the imbibing water front during TEO-free imbibition.

INTRODUCTION

A widely used assumption is that the imbibition from a fracture to the rock matrix is counter-current. The most studied experimental approach is under counter-current flow [1] - a term we here use when oil and water flows through a cross-section in opposite directions. The core plugs used for analysis are small and gravity forces are negligible compared to capillary forces, in contrast to matrix blocks in oil producing fractured reservoirs, for which the height differences in the formation will promote significant co-current flow by gravity forces. The term co-current flow implies that oil and water both flow in the same direction through the rock cross-section. Water drive will generally involve both counter-current and co-current flow in various portions of the reservoir, depending on the magnitude of capillary to gravity forces [2]. Co-current imbibition prevails if the matrix blocks are partially exposed to water, for example in gravity segregated fractures, where oil will flow preferentially towards the boundary in contact with oil [3]. Co- and counter-current imbibition may coexist during imbibition in fractured reservoirs [4], but the flows are different: counter-current flow has lower fluid mobility, lower mobile saturations (lower relative permeabilities), and higher viscous interaction between the phases [5]. Consequently, counter-current laboratory

measurements on small cores may underestimate both production rate and ultimate recovery when scaled to field conditions.

Studied Boundary Geometries

In standard experiments, core plug sample boundaries are either sealed or fully submerged in brine at all times. Several boundary conditions have been studied extensively in the literature; the most frequent are All-Faces-Open (AFO) and One-End-Open (OEO). During AFO, an oil saturated core plug, normally with an initial water phase established by forced displacement with oil, is submerged in water and the water imbibes freely. The flows are a mix of counter-current and co-current. For OEO, the curved surface of the cylindrical core and one end face are sealed and only one end face is open for flow. A partially or fully oil saturated core plug is submerged in water and spontaneous imbibition starts. For OEO only counter-current flow will occur because water enters and oil escapes through the same open end. Other, less frequently studied, boundary conditions include Two-Ends-Open (TEO) and Two-Ends-Closed (TEC), see e.g. Mason *et al.* 2009 [6]. For the TEO boundary condition, oil production can be measured separately for each end and often features asymmetry [7]. Using the TEO boundary condition in horizontally positioned core plugs, the amount of oil produced from each open end face was often unpredictably asymmetrical, even though the amount of water imbibed from each end face was equal and symmetric with respect to the center of the core (sometimes referred to as the no-flow boundary). Hence, oil was produced by both co- and counter-current imbibition, even in a short system not influenced by gravity. The experimentally observed asymmetric oil production can be explained by the need to overcome the capillary back pressure at the outlet face of the matrix.

The Capillary Back Pressure

During imbibition, the capillary back pressure is defined as the pressure difference between the non-wetting phase ($P_{nw,o}$) and the wetting phase ($P_{w,o}$) at the brine face of the porous media. The wetting phase pressure at the open face is zero. For spontaneous imbibition to progress, the imbibition pressure has to exceed the capillary back pressure required for the production of the non-wetting phase from out of the largest pores at the open face. The capillary back pressure may also be referred to as the bubble pressure [8]. It exists because the production mechanism of the non-wetting phase at the open end face is similar to a drainage process. The capillary back pressure is determined by the largest pores at the surfaces where non-wetting phase is produced as droplets [9, 10].

The asymmetric oil flows from each open end face reported by Mason *et al.* 2010 [7] was shown to occur simultaneously with symmetric influx of brine from each end as quantified by nuclear tracer imaging [11]. Hence, pore-scale heterogeneities at the rock surface, related to production paths for oil, may have a disproportionately large effect on the recovery and flow of oil, whereas water influx was much less affected by small changes in the capillary back pressure This illustrates that the properties of the fracture/matrix boundary have significant impact on the exchange of fluids between

fracture and matrix. Measurement of the simultaneous production of oil and influx of water provides an account of water and oil flow across each open end face.

Relative Permeability and Capillary Pressure from Spontaneous Imbibition

The experimentally observed asymmetrical oil production is related to the values of the capillary back pressures acting at the outlet faces of the core. A small difference in capillary back pressure between the two open end faces may consume a substantial fraction of the capillary pressure driving the flow of oil. To study the capillary back pressure in a more controlled manner, the TEO-free boundary condition was implemented, whereby one of the core faces is in contact with oil rather than water Although this boundary condition has been studied previously [5, 12], an analysis of the governing parameters, including the capillary back pressure, has only been reported recently with the M^2HF model [13, 14].

Imbibition always starts out counter-currently for the TEO-free boundary condition. How long this mode continues depends on the mobilities of the two fluids. If the mobility of the oil is high (i.e. low viscosity oil) then counter-current imbibition soon ceases and imbibition becomes co-current with production varying approximately as the square root of time. However, if the resistance is mainly in the oil phase (high oil viscosity compared with water), the resistance to co-current flow decreases over time because the distance oil has to flow to reach the oil-filled end face decrease, i.e. imbibition rate increases with time.

Two-phase flow functions can be estimated during TEO spontaneous imbibition using three simple measurements that are individually standard, but are rarely, if ever, combined. First, the ratio between counter-current flow and co-current flow for the two-ends-open free boundary condition is quantified by measuring oil production separately from each end face. Second, the pressure development during the dynamic spontaneous displacement process is measured along the length of the core using pressure transducers. Thirdly, imaging of the advancing fluid fronts are obtained during the spontaneous imbibition tests to validate the assumption that displacement is piston-like.

PROCEDURES

Positron Emission Tomography

Techniques for *in situ* visualization are vital tools for studying details of flow within opaque systems such as porous rock samples. Non-invasive, non-perturbing methods include X-ray, X-ray computed tomography (CT), nuclear tracer imaging (NTI), nuclear magnetic resonance (NMR), nuclear tracer imaging (NTI) and magnetic resonance imaging (MRI). Positron emission tomography (PET) is a frequently used explicit method for clinical oncology and clinical diagnosis, where detectors register gamma ray pairs emitted indirectly by a positron-emitting radionuclide in a tracer fluid injected into the patient. Although primarily used as a clinical diagnostic tool, PET has also more

recently been used to visualize, and partly quantify, fluid transport in geomaterials [15, 16].

In positron decay, a positron is emitted from the nucleus accompanied by an electron to balance atomic charge. After emission, the positron loses kinetic energy by interactions with the surroundings, and at near-zero momentum, the positron combines with an electron and annihilates at a finite distance outside the radioactive nucleus. The electromagnetic radiation, in the form of two 511 keV photons emitted in opposite directions to conserve momentum, is registered only if the photon pair is within the coincidence window and the line-of-response (LOR) acceptance angle [17]. PET scanners are well suited for flow studies because 511 keV photons penetrate the aluminum confinement vessel holding the rock sample at elevated pressures. For practical purposes, the beta decay is insensitive to temperature and pressure [18], making PET suitable for visualization of flow in porous rocks held under pressurized in confinement vessels.

Preparing core plugs with the TEO-FREE boundary geometry

With the TEO-free condition one end is in contact with brine and the other end in contact with oil at the same pressure. Under these circumstances brine can only enter one end of the core, but the oil can leave from either one or both ends. Ratios of oil/brine flow can be readily measured for each end. The experimental procedure using the TEO-free boundary geometry was as follows:

1. Cylindrical chalk core plugs of different lengths were cut on a lathe. Sandstone cores were drilled from quarried slabs. The core plugs surfaces were gently washed using water to remove loose particles
2. Cores were dried at room temperature for at least 24 hours before drying them in a heated oven until stable weight
3. Diameters and lengths were measured to obtain bulk volume
4. The circumference of a core was sealed by coating with a thin layer (less than 5 mm) of epoxy resin
5. An end-piece with a void was attached at one the end face (later filled with oil and serving as the oil-filled end face). The end piece was machined from polyoxymethylene (POM)

5*. With PET (or other) imaging: Attach an end piece at the inlet with void for accumulation and transport of liquids

6. Attach a short stainless steel tube at the end piece for oil production

6*. With pressure measurements: Drill a 10 mm hole into the curved surface of the epoxy-coated surface of the cylindrical core to allow insertion of a steel tube (1/8in OD). Cement the outside of the steel to the rock with epoxy.

7. Record the dry weight of the core and end piece. Saturate the core and end pieces with oil under vacuum. Check that the rock is fully saturated with oil by calculating the average porosity of the rock from the increase in weight. (The volume of the end piece and the pressure and production tubes are excluded). Core permeabilities were not measured: however, values of 3-8mD (chalk) and 1200mD (sandstone) have previously been measured.

8. To reduce "induction time" effects, start the imbibition experiments as soon as possible after filling with oil, preferably on the same day. Submerge the oil-saturated assembly in brine and record the oil produced in inverted graded funnels set at each end of the core.

Spontaneous imbibition in PET/CT

The epoxy-coated oil-filled (decane μ_o=0.74) core was placed within a rectangular Plexiglas box on the standard patient table on the combined PET/CT scanner. Pre-installed software and lasers were utilized for accurate placement of the rock system with respect to the CT gantry and the PET detector array. The rock sample was placed in the center of the bore (diameter 700 mm) to optimize CT and PET images. The rock system was stationary within PET detector array, with an axial field of view of 169 mm. Temporal resolution was determined in post processing for optimal visualization of the displacement process. Changes in pressure and volume were monitored and recorded. Radioactive 1wt% NaCl brine with water-soluble ^{18}F-FDG (μ_w=1.09 cP) was circulated through the inlet end piece using a constant rate injection pump to start the imbibition process, see Figure 1. External pressure transducers measured pressure changes during imbibition, and volumetric oil measurements were registered manually over time. Fluid saturations were found from the linear relationship between the number of disintegrations and the saturation of the labelled fluid.

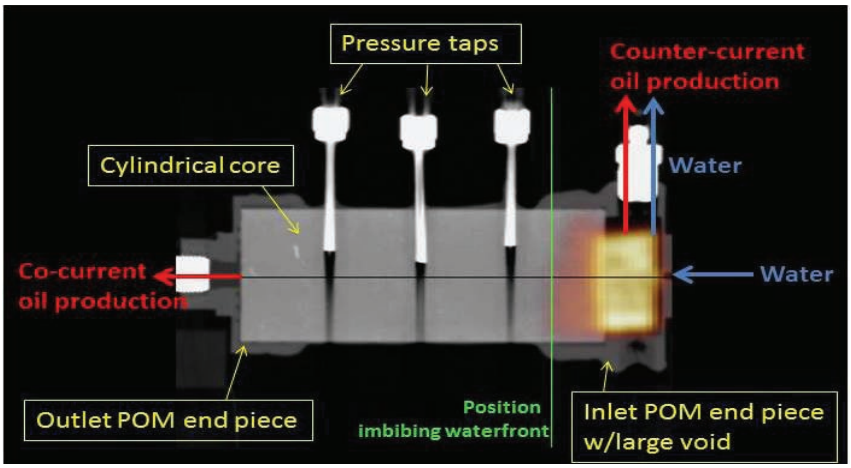

Figure 1. Experimental setup for spontaneous imbibition with PET imaging using the TEO-free boundary condition. The CT image shows a horizontal chalk plug with three pressure tappings and POM end pieces for water inflow and counter-current and co-current oil production. Volumetric measurements were performed outside the PET ring, and a cylinder pump ensured continuous cycling of water into the end piece for the duration of the test [19].

Calculating Relative Permeability and Capillary Pressure

The M^{2}HF model based on piston-like displacement was previously developed for pure 1D counter-current or co-current spontaneous imbibition [13, 14]. During co-current imbibition, the expected position of the imbibition front at time *t* can be found from

$$\frac{X_f}{L} = -D + \sqrt{D^2 + Et} \quad D > 0 \tag{1}$$

where X_f is the distance of the imbibition front (cm), L is the sample length (cm) and t is the imbibition time (min).

The constant D is defined as

$$D = \frac{1}{\left(\mu_w/k_{rw}\right)\left(k_{rnw}/\mu_{nw}\right)-1} \tag{2}$$

where μ_w is the wetting phase viscosity (mPa s), μ_{nw} is the non-wetting phase viscosity (mPa s), k_{rw} is wetting phase relative permeability *behind* the imbibition front and $k_{rnw}$is the non-wetting relative permeability *ahead* of the imbibition front.

The constant E is defined as

$$E = \frac{2KP_{c,f}}{100\varphi L^2 S_{wf}} \frac{1}{\mu_w/k_{rw} - \mu_{nw}/k_{rnw}} \tag{3}$$

where φ is the porosity, K is the absolute permeability, S_{wf} is the average wetting phase saturation behind the imbibition front, and $P_{c,f}$ is the capillary pressure at the imbibition front (kPa). Equations 1−3 can be used to calculate the distance of advance of the imbibition front if imaging is not available. In this work, local saturation measurements are measured directly with PET. The samples do not contain an initial water saturation as is usual in practice. The (k_{rnw}) ahead of the imbibition front is unity (1). The average water saturation (S_{wf}) behind the imbibition front can be obtained from the amount of oil production divided by the pore volume behind the imbibition front. Hence, there are only two unknown parameters in Eq. 2 and 3; the relative permeability to brine behind the imbibition front (k_{rw}) and the capillary pressure at the imbibition front ($P_{c,f}$).

The capillary back pressure at the open face was obtained from the oil production curve by recording the pressure at which counter-current production stops. This occurs when the non-wetting phase pressure at the front equals the capillary backpressure at the open face and there is no differential pressure to drive the non-wetting phase towards the inlet. The pressure measured with a transducer can be scaled to the pressure at the front and thus to the capillary back pressure by using simple geometry, assuming linear pressure drops,

$$P_{nw,f} = P_{c,o} = P_{nw,t} \frac{L - x_f}{L - x_t} \tag{4}$$

where $P_{nw,f}$ is the non-wetting pressure at the imbibition front, $P_{c,o}$ is the capillary back pressure at the open face, $P_{nw,f}$ is measured (oil) pressure in the transducer, and X_t the position of the transducer.

RESULTS

Figure 2 shows results using the TEO-free boundary conditions for two chalk plugs CHP26 and CHP27. The low viscosity mineral oil used (n-decane) promotes co-current

imbibition with this boundary geometry because the dominant resistance is in the aqueous phase.

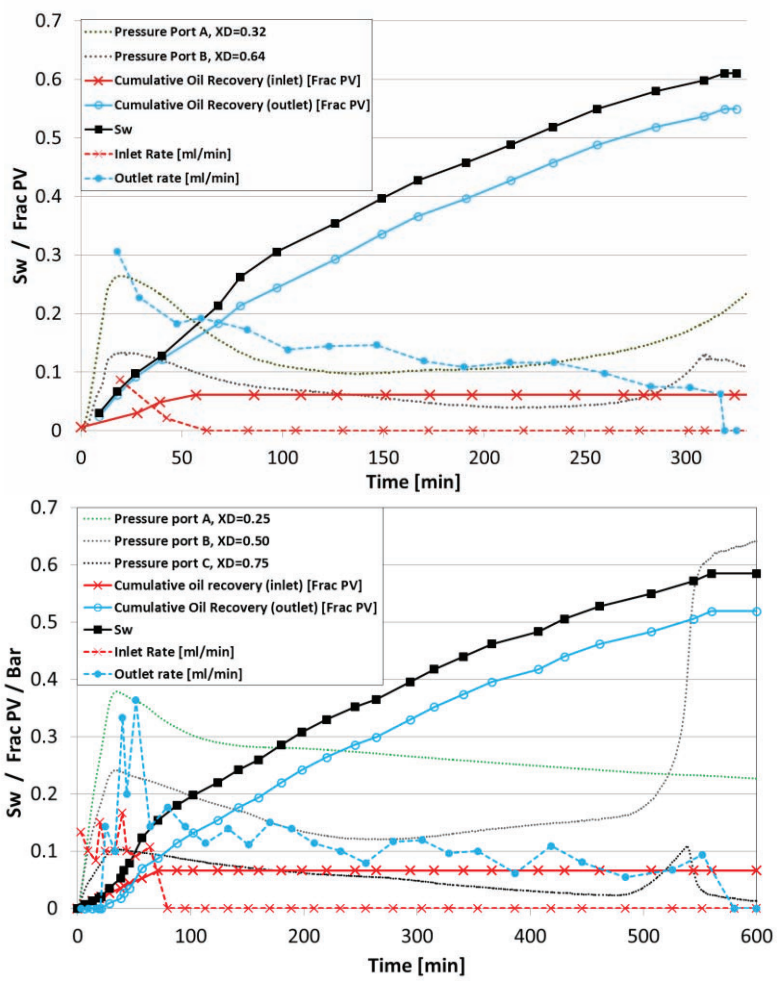

Figure 2. Spontaneous imbibition using the TEO-free boundary condition in core plugs CHP26 (top) and CHP27 (bottom). The counter-current inlet (end face in contact with brine) oil production (solid red line with crosses) was less compared to the co-current outlet (end face in contact with oil) oil production (solid blue line with open circles). Counter-current oil production was 10% for CHP26 and 11.2% for CHP27. Imbibition time increases with core length. Total production (CHP26: R_F=61 %OOIP; CHP27: R_F=58 %OOIP), with a uniform distribution. The locations of pressure ports are included for both tests. The recorded pressures are used to calculate the capillary back pressure.

Access to local water saturation during the imbibition process using PET/CT imaging allowed us to test the assumption of piston-like displacement that forms the basis for calculating relative permeability and capillary pressure from these tests. The front position can be found (without imaging) from the amount of brine imbibed (equal to the total oil produced) divided by the brine imbibed when the front reaches the end of the core. Figure 3 (left) shows these calculations for CHP26 and CHP27 versus square root of time compared to the tracked imbibition front using PET. These two independent measurements fell into alignment by the time counter-current imbibition ceases at the

inlet end. These results verify that the imbibition front is piston-like and co-current. Figure 3 (right) shows the calculated front position X_f given by Eq. 1 plotted against the experimentally measured X_f using PET. A value of D can be found that gives a straight line. From D, a value of E can be determined that gives a gradient of unity. Once the values D and E are determined, values of krw and $P_{c,f}$ are found using Eq. 2 and Eq. 3. The $P_{c,o}$ is calculated using Eq. 4. Table 1 lists relative permeabilities and capillary pressures.

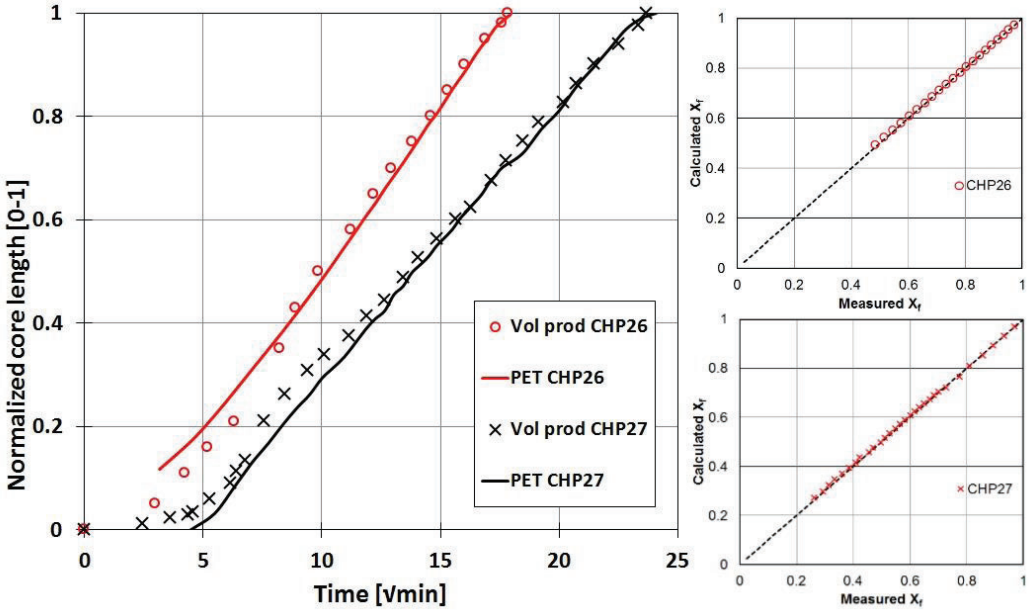

Figure 3. Left: Front position based on piston-like displacement (red open circles: CHP26; black crosses: CHP27) and visualized front position (solid red line: CHP26; solid black line: CHP27) vs. time. Right: Calculated front position (X_f) using Eq. 1 vs. measured front position using PET for core plugs CHP26 (top) and CHP27 (bottom).

Table 1. Core properties, calculated relative permeability and capillary pressures

	L [cm]	D [cm]	Por [frac]	k_{rw}	$P_{c,f}$ [kPa]	$P_{c,o}$ [kPa]	$P_{c,o}/P_{c,f}$
CHP26	8.88	5.08	0.455	0.33	64.2	21.8, 22.2	0.34
CHP27	11.8	5.08	0.468	0.31	78.2	33.7, 32.7, 28.1	0.40

Figure 4 shows the development of imbibing water (the labelled phase) during spontaneous imbibition with the TEO-free boundary geometry using PET/CT. The core is positioned horizontally during the experiment. The PET signal only measures the water and is overlaying a CT image to align with system geometries. The locations of the three pressure ports can be seen on the CT images, and appear brighter than surrounding rock due to higher density. Shadows on the CT image below the pressure ports are artefacts and does not represent areas of low CT numbers. The porosity was uniformly distributed along the length of the core. Water was injected into the void of the inlet end piece and

appears bright yellow (high intensity) on the images. Each image is an accumulation of PET signal during 10 min of imbibition and the advancing imbibition front may look slightly dispersed on the images. Figure 4 shows the position of the front at 4 selected times, and the advancing front progress as a piston.

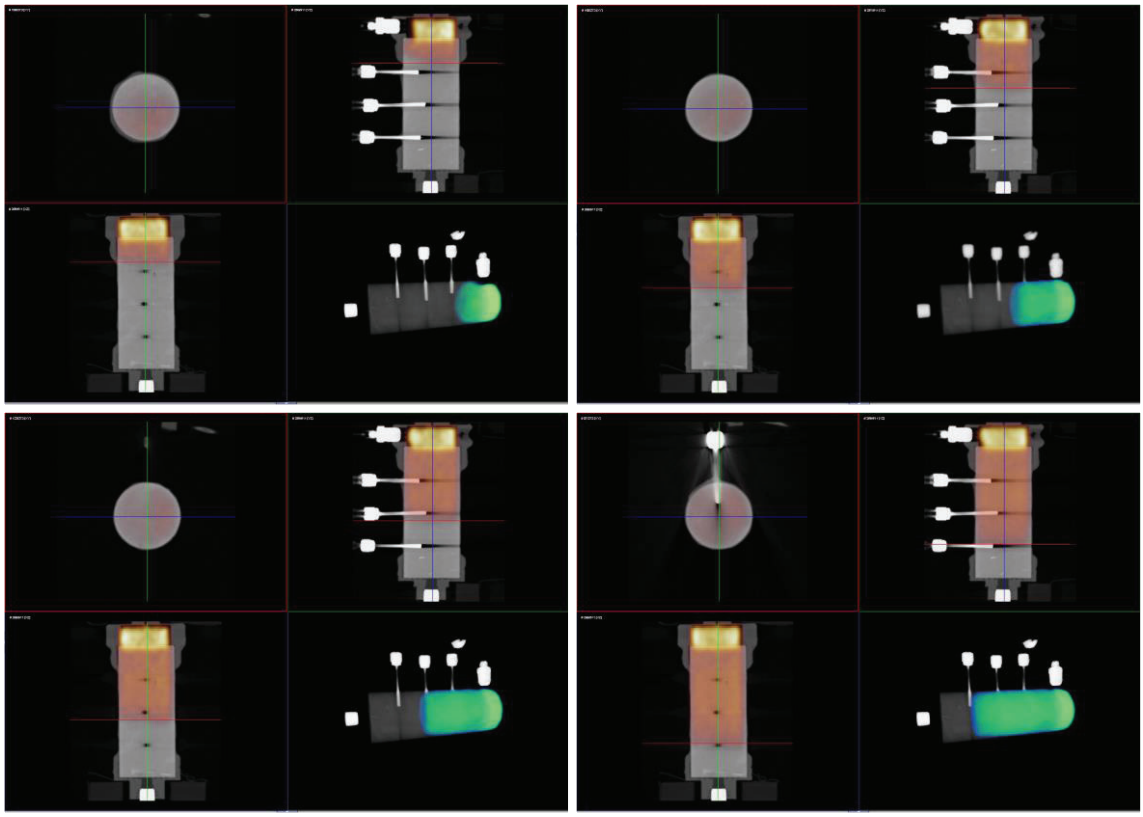

Figure 4. Qualitative PET visualization (color) overlaying CT (gray scale) of spontaneous imbibition with the TEO-free boundary condition for core plug CHP27.The location of the front is shown at four times (TOP: 40 min (left), 110min (right); BOTTOM: 200min (left), 300min (right)). Each image shows four orientations: cross-section (XY) at imbibition from (upper right); 2D slice (YZ) with pressure ports (upper left); bird eye 2D slice (XZ); and 3D image (XYZ). Colors on 2D images: high intensity (yellow) area is brine-filled void in inlet end piece; red is advancing water in core. Colors on 3D image: darker green is brine in void spacer and light green is the advancing water in the core. The water advances as a near-perfect piston from the inlet towards the outlet.

Figure 5 shows quantitative one dimensional saturation profiles for selected times during the imbibition process for core plug CHP27. The calculations are based on the PET signal and have been reduced from 3D to 1D by averaging. No additional smoothing has been applied. An assumption of uniform water distribution at the end of the test (S_w=0.58) is used to scale the normalized PET signal. We observe that this assumption was valid as the last signal intensity at the end was (within experimental uncertainty) a straight line. The front was not a perfect piston-like displacement, but the imbibition front was self-similar and maintained its shape throughout the test. The profiles slightly dispersed

because they are based on 10 min time-averaged PET images rather than snapshots of the water-distribution.

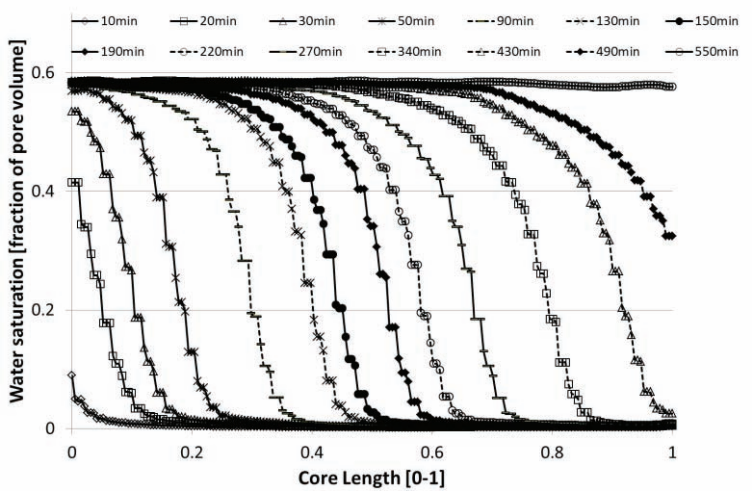

Figure 5. One dimensional water saturation profiles during TEO-free spontaneous imbibition in core plug CHP27. A sharp front advances through the core during imbibition; its shape is maintained during the displacement process.

The results in Figure 5 demonstrate the use of PET as an imaging tool for oil-water displacement in porous media with quantified local fluid saturations. Because PET relies on direct measurement of the labelled phase (water in this work) PET is superior compared to CT for determining front progression during flow injection tests and for determining spatial fluid saturation. We also learned that PET imaging has a great potential for study of low porosity samples because of the explicit fluid measurements provide high image quality and high signal to noise ratio (SNR) independent of low pore volume.

DISCUSSION

Imbibition is usually modelled by numerical solution of a set of differential equations. The solution requires functions of capillary pressure, and the relative permeabilities to both flowing phases, which are not usually known. If they are known, the values are commonly determined from separate experiments which may not be representative of flow during spontaneous imbibition [5].

A relatively straightforward mathematical analysis of co-current imbibition predicts that the volume of oil produced will depend on the square root of time. This is useful for correlation purposes. However, this behavior only allows determination of a single parameter which involves a group of core and liquid properties. The experimentally observed oil flows with the TEO-free boundary geometry, in this work and elsewhere, can only be explained by the influence of the capillary back pressure at the brine end of the core. The observation that counter-current oil production stops entirely after just 10% of total production implies that the driving pressure (the capillary pressure at the front) is

lower than some threshold. We describe this threshold as the capillary back pressure. The back pressure resists oil production because oil is produced as bubbles on the open end face during imbibition. This pressure was estimated using pressure measurements in combination with the position of the imbibing front when the counter-current production stopped. Although small in absolute value, the capillary back pressure was approximately 1/3 of the driving pressure.

Recently, the M^2HF-model [13, 14], initially developed in high-capillary chalk, was demonstrated in unconsolidated sand packs by Meng *et al.* [20]. By varying the liquid viscosity ratios, the water saturation behind the front was varied to establish a wider range of saturation on the relative permeability curve. They installed a disc with smaller pore sizes at the inlet end face in contact with water to force pure co-current imbibition. This demonstrates that the method is applicable in media for which acting capillary pressures are low. We expect the methodology to work equally well, as indicated by initial tests, in low-permeability/porosity rocks such as tight gas sands where standard core analysis is tedious and often inaccurate.

CONCLUSIONS

Using the M^2HF-model, the oil production measured separately from each end face during spontaneous imbibition using the TEO free boundary geometry can be used to estimate the relative permeability to brine behind the front and the effective capillary driving pressure at the front.

The capillary back pressure at the open face is not zero, as is commonly assumed. The capillary pressure is an essential factor in analysis of imbibition data.

The assumption of piston-like displacement during spontaneous imbibition (without initial water) was confirmed with PET imaging. We demonstrate the use of PET as a novel methodology to study flow in geomaterials, for explicit flow visualization.

REFERENCES

1. Morrow, N.R. and G. Mason, *Recovery of oil by spontaneous imbibition.* Current Opinion in Colloid & Interface Science, 2001. **6**(4): p. 321-337.
2. Bourbiaux, B.J., *Understanding the Oil Recovery Challenge of Water Drive Fractured Reservoirs*, in *International Petroleum Technology Conference*, 2009. International Petroleum Technology Conference: Doha, Qatar.
3. Pooladi-Darvish, M. and A. Firoozabadi, *Cocurrent and Countercurrent Imbibition in a Water-Wet Matrix Block.* SPE Journal, 2000. **5**(1): p. 3-11.
4. Karpyn, Z.T., P.M. Halleck, and A.S. Grader, *An experimental study of spontaneous imbibition in fractured sandstone with contrasting sedimentary layers.* Journal of Petroleum Science and Engineering, 2009. **67**: p. 48-65.
5. Bourbiaux, B.J. and F.J. Kalaydjian, *Experimental study of cocurrent and countercurrent flows in natural porous media.* SPE Reservoir Eval. & Eng., 1990. **5**: p. 361– 368.

6. Mason, G., H. Fischer, N.R. Morrow, D.W. Ruth, and S. Wo, *Effect of sample shape on counter-current spontaneous imbibition production vs time curves.* Journal of Petroleum Science and Engineering, 2009. **66**(3-4): p. 83-97.
7. Mason, G., H. Fischer, N.R. Morrow, E. Johannesen, A. Haugen, A. Graue, and M.A. Fernø, *Oil Production by Spontaneous Imbibition from Sandstone and Chalk Cylindrical Cores with Two Ends Open.* Energy & Fuels, 2010. **24**: p. 1164-1169.
8. Mason, G. and N.R. Morrow, *Developments in spontaneous imbibition and possibilities for future work.* Journal of Petroleum Science and Engineering, 2013. **110**(0): p. 268-293.
9. Li, Y., D. Ruth, G. Mason, and N.R. Morrow, *Pressures acting in counter-current spontaneous imbibition.* Journal of Petroleum Science and Engineering, 2006. **52**(1-4): p. 87-99.
10. Unsal, E., G. Mason, N.R. Morrow, and D.W. Ruth, *Bubble Snap-off and Capillary-Back Pressure during Counter-Current Spontaneous Imbibition into Model Pores.* Langmuir, 2009. **25**(6): p. 3387-3395.
11. Graue, A. and M.A. Fernø, *Water mixing during spontaneous imbibition at different boundary and wettability conditions.* Journal of Petroleum Science and Engineering, 2011. **78**(3-4): p. 586-595.
12. Dong, M., F.a.L. Dullien, and J. Zhou, *Characterization of Waterflood Saturation Profile Histories by the 'Complete' Capillary Number.* Transport in Porous Media, 1998. **31**(2): p. 213-237.
13. Haugen, A., M.A. Fernø, G. Mason, and N.R. Morrow, *The Effect of Viscosity on Relative Permeabilities Derived from Spontaneous Imbibition Tests.* Transport in Porous Media, 2015. **106**(2): p. 383-404.
14. Haugen, Å., M.A. Fernø, G. Mason, and N.R. Morrow, *Capillary pressure and relative permeability estimated from a single spontaneous imbibition test.* Journal of Petroleum Science and Engineering, 2014. **115**(0): p. 66-77.
15. Dechsiri, C., A. Ghione, F. van de Wiel, H.G. Dehling, A.M.J. Paans, and A.C. Hoffmann, *Positron emission tomography applied to fluidization engineering.* Canadian Journal of Chemical Engineering, 2005. **83**(1): p. 88-96.
16. Kulenkampff', J., M. Gruundig, M. Richter, and F. Enzmann, *Evaluation of positron-emission-tomography for visualisation of migration processes in geomaterials.* Physics and Chemistry of the Earth, 2008. **33**(14-16): p. 937-942.
17. Bailey, D.L., D.W. Townsend, P.E. Valk, and M.N. Maisey, eds. *Positron Emission Tomography*. Basic Sciences. 2005, Springer.
18. Emery, G.T., *Perturbation of Nuclear Decay Rates.* Annual Review of Nuclear Science, 1972. **22**(1): p. 165-202.
19. Fernø, M.A., Å. Haugen, G. Mason, and N.R. Morrow. *Spontaneous Imbibition Revisited: A New Method to Determine Kr and Pc by Inclusion of the Capillary Backpressure* at *IOR 2015 – 18thEuropean Symposium on Improved Oil Recovery*, Dresden, Germany, 14-16 April, 2015.
20. Meng, Q., H. Liu, and J. Wang, *Entrapment of the Non-wetting Phase during Co-current Spontaneous Imbibition.* Energy & Fuels, 2015. **29**(2): p. 686-694.